

First X-ray Characterization and Theoretical Study of π -Alkyne, Alkynyl-Hydride, and Vinylidene Isomers for the Same Transition Metal Fragment $[\text{Cp}^*\text{Ru}(\text{PEt}_3)_2]^+$

Emilio Bustelo, Jorge J. Carbó,[†] Agustí Lledós,[†] Kurt Mereiter,[‡]
M. Carmen Puerta, and Pedro Valerga*

Contribution from the Departamento de Ciencia de los Materiales, Ingeniería Metalúrgica y Química Inorgánica, Universidad de Cádiz, Apdo. 40, 11510 Puerto Real, Cádiz, Spain, Departament de Química, Universitat Autònoma de Barcelona, 08193 Bellaterra, Barcelona, Spain, and Institute of Chemical Technologies and Analytics, Vienna University of Technology, Getreidemarkt 9, A-1060 Vienna, Austria

Received October 28, 2002; Revised Manuscript Received January 14, 2003; E-mail: pedro.valerga@uca.es

Abstract: The reaction of the chloro-complex $[\text{Cp}^*\text{RuCl}(\text{PEt}_3)_2]$ with acetylene gas in methanol gave the π -alkyne complex $[\text{Cp}^*\text{Ru}(\eta^2\text{-HC}\equiv\text{CH})(\text{PEt}_3)_2][\text{BPh}_4]$ (**1**), which has been structurally characterized by X-ray analysis. The alkyne complex undergoes spontaneous isomerization even at low temperature, yielding the metastable alkynyl-hydride complex $[\text{Cp}^*\text{Ru}(\text{H})(\text{C}\equiv\text{CH})(\text{PEt}_3)_2][\text{BPh}_4]$ (**2**), as the result of the oxidative addition of the alkyne C–H bond. This compound has also been structurally characterized despite it tautomerizes spontaneously into the stable primary vinylidene $[\text{Cp}^*\text{Ru}(=\text{C}=\text{CH}_2)(\text{PEt}_3)_2][\text{BPh}_4]$ (**3**). This species has been alternatively prepared by a two-step deprotonation/protonation synthesis from the π -alkyne complex. Moreover, the reaction of the initial chloro-complex with monosubstituted alkynes $\text{HC}\equiv\text{CR}$ ($\text{R} = \text{SiMe}_3, \text{Ph}, \text{COOMe}, \text{tBu}$) has been studied without detection of π -alkyne intermediates. Instead of this, alkynyl-hydride complexes were obtained in good yields. They also rearrange to the corresponding substituted vinylidenes. In the case of $\text{R} = \text{SiMe}_3$, the isomerization takes place followed by desilylation, yielding the primary vinylidene complex. X-ray crystal structures of the vinylidene complexes $[\text{Cp}^*\text{Ru}(=\text{C}=\text{CH}_2)(\text{PEt}_3)_2][\text{BPh}_4]$ (**3**) and $[\text{Cp}^*\text{Ru}(=\text{C}=\text{CHCOOMe})(\text{PEt}_3)_2][\text{BPh}_4]$ (**10**) have also been determined. Both, full ab initio and quantum mechanics/molecular mechanics (QM/MM) calculations were carried out, respectively, on the model system $[\text{CpRu}(\text{C}_2\text{H}_2)(\text{PH}_3)_2]^+$ (**A**) and the real complex $[\text{Cp}^*\text{Ru}(\text{C}_2\text{H}_2)(\text{PEt}_3)_2]^+$ (**B**) to analyze the steric and electronic influence of ligands on the structures and relative energies of the three C_2H_2 isomers. QM/MM calculations have been employed to evaluate the role of the steric effects of real ligands, whereas full ab initio energy calculations on the optimized QM/MM model have allowed recovering the electronic effects of ligands. Additional pure quantum mechanics calculations on $[\text{Cp}^*\text{Ru}(\text{C}_2\text{H}_2)(\text{PH}_3)_2]^+$ (**C**) and $[\text{CpRu}(\text{C}_2\text{H}_2)(\text{PMe}_3)_2]^+$ (**D**) model systems have been performed to analyze in more detail the effects of different ligands. Calculations have shown that the steric effects induced by the presence of bulky substituents in phosphine ligand are responsible for experimentally observed alkyne distortion and for relative destabilization of the alkyne isomer. Moreover, increasing the phosphine basicity and σ donor capabilities of ligands causes a relative stabilization of an alkynyl-hydride isomer. The combination of both steric and electronic effects, makes alkyne and alkynyl-hydride isomers to be close in energy, leading to the isolation of both complexes.

Introduction

Activation of alkynes by transition-metal complexes has attracted considerable attention during the past few decades. In this context, Ru-catalyzed reactions of alkynes and related stoichiometric reactions have been extensively developed.¹ In the last years, the acetylene-vinylidene rearrangement has gained

a renewed interest coming from both experimental and theoretical points of view. In particular, some well-known complexes have been revisited. Such is the case with $[\text{CpMn}(\text{C}_2\text{H}_2)(\text{CO})_2]^2$ or $[(\text{PP}_3)\text{Co}(\text{C}_2\text{H}_2)]^+$ ($\text{PP}_3 = \text{P}(\text{CH}_2\text{CH}_2\text{PPh}_2)_3$),³ and even new insights for the free rearrangement of acetylene have been reported.⁴ The study of the alkyne-vinylidene isomerization is constantly broadened toward systems with different metals⁵ or

[†] Universitat Autònoma de Barcelona.

[‡] Vienna University of Technology.

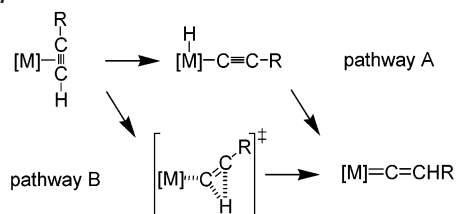
(1) For recent reviews, see: (a) Naota, T.; Takaya, H.; Murahashi, S.-I. *Chem. Rev.* **1998**, *98*, 2599. (b) Bruneau, C.; Dixneuf, P. H. *Acc. Chem. Res.* **1999**, *32*, 311. (c) Puerta, M. C.; Valerga, P. *Coord. Chem. Rev.* **1999**, *193–195*, 977. (d) Trost, B. M.; Toste, D.; Pinkerton, A. B. *Chem. Rev.* **2001**, *101*, 2067. (e) Ritleng, V.; Sirlin, C.; Pfeffer, M. *Chem. Rev.* **2002**, *102*, 1731.

(2) (a) Silvestre, J.; Hoffmann, R. *Helv. Chim. Acta* **1985**, *68*, 1461. (b) De Angelis, F.; Sgamellotti, A.; Re, N. *Organometallics* **2002**, *21*, 2715.

(3) (a) Bianchini, C.; Peruzzini, M.; Vacca, A.; Zanolini, F. *Organometallics* **1991**, *10*, 3697. (b) Pérez-Carreño, E.; Paoli, P.; Ienco, A.; Mealli, C. *Eur. J. Inorg. Chem.* **1999**, *8*, 1315.

(4) Hayes, R. L.; Fattal, E.; Govind, N.; Carter, E. A. *J. Am. Chem. Soc.* **2001**, *123*, 641.

Scheme 1



with new auxiliary ligands.⁶ In the case of Ru and Os complexes a number of papers dealing with the role of the metallic fragment, auxiliary ligands or alkyne substituents on such process, has been reported.^{6–8}

The isomerization mechanism into vinylidene has been proposed to proceed via π -alkyne intermediates although they are seldom isolated or even detected. The ulterior tautomerization may occur through two alternative pathways (Scheme 1). A first reasonable approach involves an active role of the metal center, which undergoes the oxidative addition of the alkyne, furnishing an intermediate alkyne-hydride complex (Scheme 1-A). This pathway is competitive with a direct 1,2-hydrogen shift in the former alkyne complex (Scheme 1-B), depending on the particular metallic fragment. The second of these mechanisms seems to predominate within the ruthenium chemistry. A direct isomerization of this type has been described by Selegue et al, reporting the first structurally characterized pair of C_2H_2 isomers, namely π -alkyne and vinylidene.⁹ On the other hand, several examples and ab initio MO calculations support the mechanism through alkyne-hydride intermediates in the chemistry of Co,³ Rh and Ir.¹⁰

Our contribution to this field started from the isolation of the first ruthenium alkyne-hydride complex $[\text{Cp}^*\text{Ru}(\text{H})(\text{C}\equiv\text{CR})(\text{dippe})]^+$ (dippe = 1,2-bis(diisopropylphosphine)ethane), as metastable intermediate in the synthesis of the corresponding vinylidene isomer.¹¹ This result has been extended to a number of alkynes and alkynols.¹² The substitution of the diphosphine dippe for two monodentate phosphine ligands such

as PEt_3 , gave similar results in reaction with alkynols.¹³ The present paper describes new outcomes from the activation of acetylene and 1-alkynes with $[\text{Cp}^*\text{RuCl}(\text{PEt}_3)_2]$, and reports the X-ray structural characterization of π -alkyne, alkyne-hydride, and vinylidene isomers. To the best of our knowledge, this is the first time that those three C_2H_2 isomers have been structurally characterized for the same transition metal complex and the same alkyne. Besides that, we have carried out pure quantum mechanics (QM) calculations on the $[\text{Cp}^*\text{Ru}(\text{C}_2\text{H}_2)(\text{PH}_3)_2]^+$ (A) model system. We have combined the pure quantum mechanics calculations with quantum mechanics/molecular mechanics (QM/MM) calculation on the $[\text{Cp}^*\text{Ru}(\text{C}_2\text{H}_2)(\text{PET}_3)_2]^+$ (B) real system in order to assess the steric effects of real ligands. Furthermore, full ab initio energy calculations on the optimized QM/MM model have been performed to recover the electronic effect of real ligands. Additionally, pure quantum mechanics calculations on $[\text{Cp}^*\text{Ru}(\text{C}_2\text{H}_2)(\text{PH}_3)_2]^+$ (C) and $[\text{Cp}^*\text{Ru}(\text{C}_2\text{H}_2)(\text{PMe}_3)_2]^+$ (D) models have been employed to analyze in more detail the effects of the different ligands. The combination of methods and model systems has allowed us to separate, identify and evaluate the different effects of ligands on the structure and relative energies of the three C_2H_2 isomers. Thus, the theoretical study has focused on the structural and energetic properties of these three isomers, whereas the detailed kinetic study of the alkyne-vinylidene isomerization is out of the purpose of the current work.

Results and Discussion

Synthesis and Characterization of π -Alkyne, Alkyne-Hydride and Vinylidene Species. Acetylene Activation. In our previous studies, the isolation of metastable alkyne-hydride intermediates has been possible due to the high insolubility of these cationic complexes as BPh_4 salt in MeOH.^{11–13} Thus, the reaction of $[\text{Cp}^*\text{RuCl}(\text{PEt}_3)_2]$ and acetylene has been carried out by bubbling acetylene gas through a NaBPh_4 solution in MeOH, to which the chloro-complex was finally added. This sequence causes the immediate precipitation of the yellow compound $[\text{Cp}^*\text{Ru}(\eta^2\text{-HC}\equiv\text{CH})(\text{PEt}_3)_2][\text{BPh}_4]$ (**1**), in 85% yield. Complex **1** is stable in the solid state at room temperature. The IR spectrum exhibits the $\nu(\text{C}\equiv\text{C})$ band at 1732 cm^{-1} . The NMR spectra were recorded at $-20\text{ }^\circ\text{C}$ to prevent isomerization, displaying phosphorus-coupled triplets at 4.38 and 66.14 ppm for the C_2H_2 unit in the ^1H and $^{13}\text{C}\{^1\text{H}\}$ spectra, respectively.

In solution, compound **1** rearranges spontaneously at temperatures above $-20\text{ }^\circ\text{C}$. The process has been monitored by $^31\text{P}\{^1\text{H}\}$ NMR at $-10\text{ }^\circ\text{C}$ and the initial signal at 23.8 ppm was slowly replaced by a new one at 37.7 ppm, corresponding to the alkyne-hydride isomer described later. This fact explains why the recrystallization of **1** from an acetone/ethanol mixture at low temperature yielded a major amount of crystals of the second isomer. However, among them it was possible to identify and separate a minor amount of crystals of complex **1** (with the same color but slightly different shape). The X-ray structure of **1** has been determined, being one of the scarce half-sandwich ruthenium alkyne complexes structurally characterized.^{9,14} An

- (5) (a) (Nb): García Yebra, C.; López Mardomingo, C.; Fajardo, M.; Antiñolo, A.; Otero, A.; Rodríguez, A.; Vallat, A.; Lucas, D.; Mugnier, Y.; Carbó, J. J.; Lledós, A.; Bo, C. *Organometallics* **2000**, *19*, 1749. (b) (W): Stegmann, R.; Frenking, G. *Organometallics* **1998**, *17*, 2089. (c) (Ta): Gibson, V. C.; Parkin, G.; Bercaw, J. E. *Organometallics* **1991**, *10*, 220. (d) (Cr): Bartlett, I. M.; Connelly, N. G.; Martin, A. J.; Orpen, A. G.; Paget, T. J.; Rieger, A. L.; Rieger, P. H. *J. Chem. Soc., Dalton Trans.* **1999**, 691. (e) (Pt): Ara, I.; Berenguer, J. R.; Eguizabal, E.; Forniés, J.; Gómez, J.; Lalinde, E.; Sáez-Rocher, J. M. *Organometallics* **2000**, *19*, 4385.
- (6) Katayama, H.; Wada, C.; Taniguchi, K.; Ozawa, F. *Organometallics* **2002**, *21*, 3285.
- (7) (Ru): (a) Wakatsuki, Y.; Koga, N.; Yamazaki, H.; Morokuma, K. *J. Am. Chem. Soc.* **1994**, *116*, 8105. (b) Cadierno, V.; Gamasa, M. P.; Gimeno, J.; Pérez-Carreño, E.; García-Granda, S. *Organometallics* **1999**, *18*, 2821. (c) Cadierno, V.; Gamasa, M. P.; Gimeno, J.; González-Bernardo, C.; Pérez-Carreño, E.; García-Granda, S. *Organometallics* **2001**, *20*, 5177. (d) Tokunaga, M.; Suzuki, T.; Koga, N.; Fukushima, T.; Horiuchi, A.; Wakatsuki, Y. *J. Am. Chem. Soc.* **2001**, *123*, 11917. (e) De Angelis, F.; Sgamellotti, A.; Re, N. *Organometallics*, **2002**, *21*, 5944.
- (8) (Os): (a) Esteruelas, M. A.; López, A. M.; Ruiz, N.; Tolosa, J. I. *Organometallics* **1997**, *16*, 4657. (b) Crochet, P.; Esteruelas, M. A.; López, A. M.; Ruiz, N.; Tolosa, J. I. *Organometallics* **1998**, *17*, 3479. (c) Oliván, M.; Clot, E.; Eisenstein, O.; Caulton, K. G. *Organometallics* **1998**, *17*, 3091. (d) Baya, M.; Crochet, P.; Esteruelas, M. A.; Gutiérrez-Puebla, E.; López, A. M.; Modrego, J.; Oñate, E.; Vela, N. *Organometallics* **2000**, *19*, 2585. (e) Baya, M.; Crochet, P.; Esteruelas, M. A.; López, A. M.; Modrego, J.; Oñate, E. *Organometallics* **2001**, *20*, 4291.
- (9) Lompreg, J. R.; Selegue, J. P. *J. Am. Chem. Soc.* **1992**, *114*, 5518.
- (10) (a) Werner, H. *J. Organomet. Chem.* **1994**, *475*, 45. (b) Werner, H.; Baum, M.; Schneider, D.; Windmüller, B. *Organometallics* **1994**, *13*, 1089. (c) H. Werner, R. W. Lass, O. Gevert, J. Wolf. *Organometallics* **1997**, *16*, 4077. (d) Wakatsuki, Y.; Koga, N.; Werner, H.; Morokuma, K. *J. Am. Chem. Soc.* **1997**, *119*, 360.
- (11) de los Ríos, I.; Jiménez-Tenorio, M.; Puerta, M. C.; Valerga, P. *J. Am. Chem. Soc.* **1997**, *119*, 6529.

- (12) (a) Bustelo, E.; de los Ríos, I.; Jiménez-Tenorio, M.; Puerta, M. C.; Valerga, P. *Monatsh. Chem.* **2000**, *131*, 1311. (b) Bustelo, E.; Jiménez-Tenorio, M.; Puerta, M. C.; Valerga, P. *Eur. J. Inorg. Chem.* **2001**, 2391.
- (13) (a) Bustelo, E.; Jiménez-Tenorio, M.; Puerta, M. C.; Valerga, P. *Organometallics* **1999**, *18*, 950. (b) Bustelo, E.; Jiménez-Tenorio, M.; Puerta, M. C.; Valerga, P. *Organometallics* **1999**, *18*, 4563.

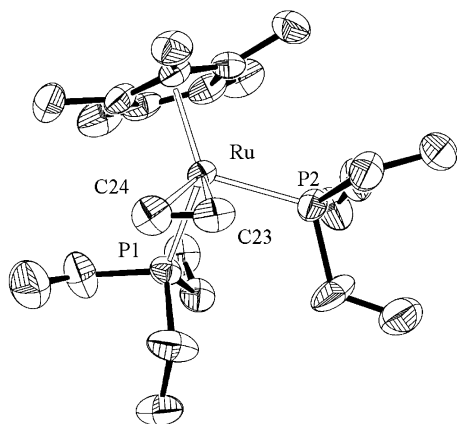


Figure 1. ORTEP drawing (50% thermal ellipsoids) of the cation $[\text{Cp}^*\text{Ru}(\eta^2\text{-HC}\equiv\text{CH})(\text{PEt}_3)_2]^+$ (**1**).

Table 1. Selected Bond Lengths (Å) for Compounds **1**, **2**, and **3** with Estimated Standard Deviations in Parentheses

bond distances (Å)					
1		2		3	
Ru(1)	P(1)	2.343(1)	Ru(1)	P(1)	2.346(1)
Ru(1)	P(2)	2.347(1)	Ru(1)	P(2)	2.328(1)
Ru(1)	C(23)	2.182(4)	Ru(1)	C(23)	2.034(4)
Ru(1)	C(24)	2.180(5)	C(23)	C(24)	1.150(6)
C(23)	C(24)	1.220(7)	Ru(1)	H(1)	1.33(4)
Ru(1)	P(1)	2.350(2)	Ru(1)	P(2)	2.335(2)
Ru(1)	C(1)	1.835(8)	Ru(1)	C(2)	1.296(11)

ORTEP¹⁵ view of the cationic complex **1** is depicted in Figure 1. Selected bond lengths and angles are listed in Tables 1 and 2.

The geometry around the ruthenium atom in **1** can be described as a three-legged piano-stool. The alkyne ligand is symmetrically bound to the ruthenium atom (2.180(5) and 2.182(4) Å). The C(23)–C(24) distance (1.220(7) Å) is slightly longer than the average value in free alkynes (1.18 Å).¹⁶

The rotational orientation of the alkyne unit relative to the $[\text{Cp}^*\text{Ru}(\text{PEt}_3)_2]$ moiety is not orthogonal to the idealized mirror plane (see Figure 2), although such disposition has been predicted by qualitative MO reasoning.¹⁷ Therefore, the torsion angles Cp–Ru–Mp–C(23) or Cp–Ru–Mp–C(24) (Cp, ring centroid; Mp, alkyne C≡C midpoint) of 69.3° and –110.7° are far from an ideally perpendicular alkyne (90° and –90°). This situation, although less pronounced, has also been reported by Selegue et al. for the complex $[\text{CpRu}(\eta^2\text{-HC}\equiv\text{CH})(\text{PMe}_2\text{-Ph})_2]^+$ (98.5° and –81.5°).⁹ Discussions on the reason of the discrepancy will be provided later on the basis of theoretical calculations.

The alkynyl-hydride complex $[\text{Cp}^*\text{Ru}(\text{H})(\text{C}\equiv\text{CH})(\text{PEt}_3)_2][\text{BPh}_4]$ (**2**) has been prepared by spontaneous isomerization of **1** at temperatures below 10 °C, to prevent the ulterior isomerization into the thermodynamically favored vinylidene isomer. Thus, compound **2** was obtained as a pale yellow solid in quantitative yield. It exhibits the $\nu(\text{C}\equiv\text{C})$ and $\nu(\text{Ru}-\text{H})$ bands at 1967 and 1935 cm^{-1} , respectively in the IR spectrum. The

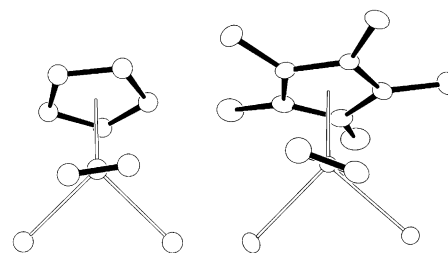


Figure 2. Alkyne rotational orientation in $[\text{CpRu}(\text{PMe}_2\text{Ph})_2]^+$ ⁹ and $[\text{Cp}^*\text{Ru}(\text{PEt}_3)_2]^+$ (**1**).

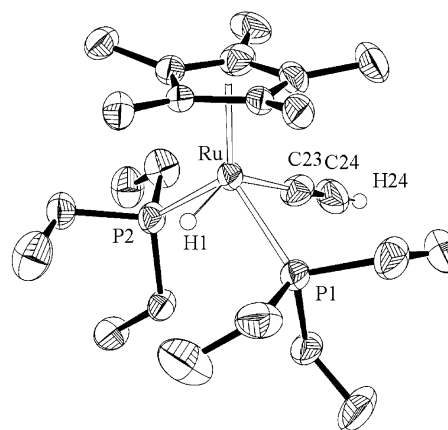


Figure 3. ORTEP drawing (50% thermal ellipsoids) of $[\text{Cp}^*\text{Ru}(\text{H})(\text{C}\equiv\text{CH})(\text{PEt}_3)_2]^+$ (**2**).

³¹P{¹H} NMR spectrum, recorded in CDCl₃ at 5 °C, consists of a singlet at 37.7 ppm. The hydride ligand appears in the ¹H NMR spectrum as a triplet at –9.27 ppm with a coupling constant of 29.5 Hz, whereas the terminal alkynyl hydrogen gives rise to a triplet at 2.09 ppm (⁴J_{HP} = 2.7 Hz). In the ¹³C-{¹H} NMR spectrum, a triplet at 93.09 ppm and a singlet at 102.1 ppm match well with the resonances expected for α and β carbons of the alkynyl ligand. Yellow crystals corresponding to the alkynyl-hydride isomer were obtained from the recrystallization of **1** as described previously. Figure 3 shows the X-ray structure of **2**. Selected bond distances and angles are listed in Tables 1 and 2.

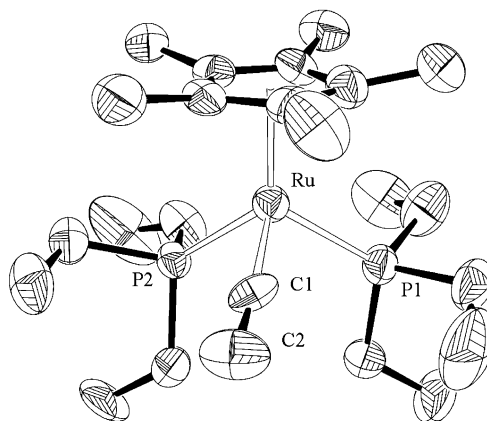
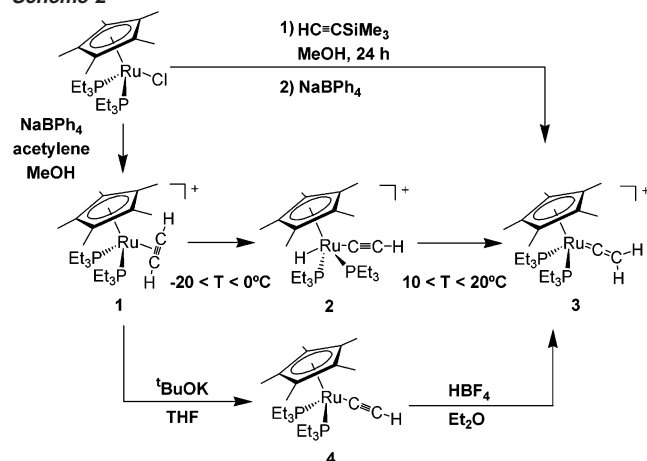
The geometry around the ruthenium atom in the cationic complex **2** can be described as a four-legged piano-stool, where the hydride and alkynyl ligands are in transoid disposition with a C(23)–Ru–H(1) angle of 131.3(16)°. The alkynyl ligand is almost linearly assembled to ruthenium, being the Ru–C(23)–C(24) angle 178.2(4)°. The P(1)–Ru–P(2) angle of 107.20(4)° is higher than that found for the analogous complex with the chelating phosphine dippe (87.5°).¹¹ The distances Ru–C(23) (2.034(4) Å) and C(23)–C(24) (1.150(6) Å) correspond to a single and triple bond, respectively.

The alkynyl-hydride complex **2** rearranges spontaneously to the vinylidene isomer. In the solid state such process occurs very slowly at room temperature, as observed for the analogous alkynyl-hydride complex with the diphosphine dippe.^{12a} In solution, the process takes place perceptibly at temperatures above 10 °C. Unfortunately, a clean synthesis of the vinylidene is not possible when temperature reaches 20 °C. Otherwise, a mixture of uncharacterized products is obtained probably owing to side-reactions coming from the reactivity of the alkynyl terminal hydrogen.

- (14) (a) Bullock, R. M. *J. Chem. Soc., Chem. Commun.* **1989**, 165. (b) Urtel, K.; Frick, A.; Huttner, G.; Zsolnai, L.; Kircher, P.; Rutsch, P.; Kaifer, E.; Jacobi, A. *Eur. J. Inorg. Chem.* **2000**, 33.
 (15) Johnson, C. K. ORTEP, *A Thermal Ellipsoid Plotting Program*; Oak Ridge National Laboratory: Oak Ridge, Tennessee, 1965.
 (16) Allen, F. H.; Kennard, O.; Watson, D. G.; Brammer, L.; Orpen, A. G.; Taylor, R. *J. Chem. Soc., Perkin Trans.* **1987**, S1.
 (17) Schilling, B. E. R.; Hoffmann, R.; Lichtenberger, D. L. *J. Am. Chem. Soc.* **1979**, *101*, 585.

Table 2. Selected Angles (deg) for Compounds **1**, **2**, and **3** with Estimated Standard Deviations in Parentheses

		bond angles (deg)			
1		2		3	
P(1)Ru(1)P(2)	93.67(4)	P(1)Ru(1)P(2)	107.20(4)	P(1)Ru(1)P(2)	96.85(7)
P(1)Ru(1)C(24)	81.28(13)	P(1)Ru(1)C(23)	79.93(12)	P(1)Ru(1)C(1)	87.6(3)
P(2)Ru(1)C(23)	79.87(14)	P(2)Ru(1)C(23)	84.19(14)	P(2)Ru(1)C(1)	94.3(3)
C(23)Ru(1)C(24)	32.47(19)	Ru(1)C(23)C(24)	178.2(4)	Ru(1)C(1)C(2)	171.8(8)
		C(23)Ru(1)H(1)	131.3(16)		

Scheme 2**Figure 4.** ORTEP drawing (50% thermal ellipsoids) of $[\text{Cp}^*\text{Ru}(\text{=C}=\text{CH}_2)(\text{PEt}_3)_2]^+$ (**3**).

An alternative procedure has been employed to prepare the primary vinylidene $[\text{Cp}^*\text{Ru}(\text{=C}=\text{CH}_2)(\text{PEt}_3)_2][\text{BF}_4]$ (**3**) by the stepwise deprotonation and protonation of **1**. Treatment of **1** with $t\text{BuOK}$ yielded the neutral alkynyl complex $[\text{Cp}^*\text{Ru}(\text{C}\equiv\text{CH})(\text{PEt}_3)_2]$ (**4**) as a yellow solid. The IR $\nu(\text{C}\equiv\text{C})$ band appears at 1942 cm^{-1} . The NMR spectra display a triplet for the alkynyl proton at 2.05 ppm, and a triplet and a singlet for the alkynyl carbons at 108.9 and 91.29 ppm, respectively. Protonation of **4** with $\text{HBF}_4\cdot\text{Et}_2\text{O}$ occurs selectively on the alkynyl β carbon atom, giving exclusively the vinylidene isomer **3**. However, the most convenient method for the preparation of **3** is the direct activation of trimethylsilylacetylene by $[\text{Cp}^*\text{RuCl}(\text{PEt}_3)_2]$. Therefore, complex **3** can be prepared in one step with 90% yield as a BPh_4 salt. A summary of the preparative procedures of complexes **1**–**4** is depicted in Scheme 2.

Recrystallization of complex **3** yielded orange crystals suitable for XRD analysis and the crystalline structure was determined, thereby completing the characterization of the isomers triad: alkyne, alkynyl-hydride, and vinylidene. Figure 4 shows an ORTEP view of the cationic complex **3**. Selected bond lengths and angles are listed in Tables 1 and 2.

The geometry around the ruthenium center can be described as a three-legged piano-stool. The distances $\text{Ru}-\text{C}(1)$ of 1.835(8) Å and $\text{C}(1)-\text{C}(2)$ of 1.296(11) Å, are typical values for a vinylidene ligand, which is almost linearly assembled to ruthenium ($\text{Ru}-\text{C}(1)-\text{C}(2)$ 171.8(8)°). The angle $\text{P}(1)-\text{Ru}-\text{P}(2)$ of 96.85(7)° is slightly higher than in the alkyne complex **1** (93.67(4)°) due to the lesser steric requirements of the vinylidene. The IR spectrum of **3** exhibits a strong absorption at 1611 cm^{-1} . In the ^1H NMR spectrum, the vinylidene protons appear at 3.57 ppm as a phosphorus-coupled triplet ($^4J_{\text{HP}} = 1.8\text{ Hz}$). The α carbon is found at 345.9 ppm as a triplet with 21.5 Hz of coupling constant, whereas the β carbon gives rise to a singlet at 102.9 ppm in the $^{13}\text{C}\{^1\text{H}\}$ NMR.

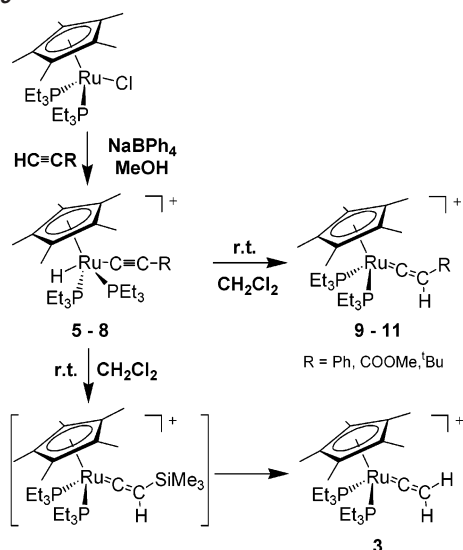
The isolation and structural characterization of the three isomers for the same transition metal fragment, resulting from the acetylene activation by $[\text{Cp}^*\text{RuCl}(\text{PEt}_3)_2]$, is particularly noteworthy because the relative stabilities of such species are usually opposed. Thus, in electron-rich complexes, the vinylidene is the most stable isomer and even the detection of any intermediate species is not possible. This is very clear in the case of the alkyne isomer, which is always proposed as a necessary intermediate in the isomerization process to vinylidene. However, they are seldom isolated as the kinetic product only when small alkyne substituents and small ancillary ligands on the ruthenium are present.^{9,14a} Data from a DFT analysis on the three isomers relative energies will be provided and discussed later.

Activation of 1-Alkynes. The activation of a number of 1-alkynes by $[\text{Cp}^*\text{RuCl}(\text{PEt}_3)_2]$ leads directly to the alkynyl-hydride complexes $[\text{Cp}^*\text{Ru}(\text{H})(\text{C}\equiv\text{CR})(\text{PEt}_3)_2][\text{BPh}_4]$ ($\text{R} = \text{SiMe}_3$ (**5**), Ph (**6**), COOMe (**7**), $t\text{Bu}$ (**8**)). Attempts to detect by $^31\text{P}\{^1\text{H}\}$ NMR the initial formation in solution of π -1-alkyne species failed.

The preparation of **5**–**8** has been carried out by a method analogous to that described in the synthesis of **1** (see Scheme 3). The presence of NaBPh_4 causes the immediate precipitation of a pale yellow solid in MeOH, avoiding the isomerization to the most stable vinylidene isomer. The IR spectra show in all cases a strong absorption around 2100 cm^{-1} , corresponding to the alkynyl $\nu(\text{C}\equiv\text{C})$ band. The ^1H NMR spectra exhibit a triplet around -9.10 ppm for the hydride ligand, with coupling constants of 27–30 Hz. In the $^{13}\text{C}\{^1\text{H}\}$ NMR spectra of **5**–**7**, signals for the alkynyl α and β carbons appear in the range 100–122 ppm.

The tautomerization process resembles to a great extent to that observed for the activation of 1-alkynes by $[\text{Cp}^*\text{RuCl}(\text{dippe})]$:^{11,12} the isomerization rate depends on the alkyne substituent, being $\text{R} = \text{COOEt} < \text{Ph} < \text{SiMe}_3 < t\text{Bu}$ (according

Scheme 3



to this, complex **8** has only been obtained as a minor product besides its vinylidene isomer); these compounds rearrange spontaneously in the solid state to vinylidene so that they must be stored below room temperature. On the other hand, the isomerization takes place slower in complexes with PEt_3 than in those with dippe , as it has been previously observed in the interaction of $[\text{Cp}^*\text{RuCl}(\text{PEt}_3)_2]$ with alkynols.¹³

The vinylidene complexes $[\text{Cp}^*\text{Ru}(\text{C}=\text{CHR})(\text{PEt}_3)_2][\text{BPh}_4]$ (R = Ph (**9**), COOMe (**10**), ^tBu(**11**)) have been obtained by stirring a solution of $[\text{Cp}^*\text{RuCl}(\text{PEt}_3)_2]$ and the corresponding alkyne for 6 h in MeOH. The subsequent addition of NaBPh₄ causes the precipitation of an orange microcrystalline solid. The IR spectra show a strong and broad vinylidene absorption in the range 1620–1700 cm^{-1} . The vinylidene proton appears at 5.12, 4.70, and 3.72, respectively for compounds **9**–**11** in the ¹H NMR spectra. The ¹³C{¹H} NMR signal for the vinylidene α carbon appears around 345 ppm. Recrystallization of **10** gave orange crystals suitable for X-ray structural analysis. An ORTEP view of the cationic complex is depicted in Figure 5. Selected bond lengths and angles are listed in Table 3.

The distances Ru–C(11) (1.806(8) Å) and C(11)–C(12) (1.308(10) Å) are quite similar to those observed for the primary vinylidene complex **3** (1.835(8) Å and 1.296(11) Å). Likewise the atoms Ru–C(11)–C(12) (175.4(6)°) are almost linearly arranged. All angles around C(12) and C(13) are close to 120°, in agreement with a sp^2 hybridization.

Finally, the isomerization of the alkynyl-hydride complex **5** (R = SiMe₃) to vinylidene occurs followed by an immediate desilylation process, leading directly to the formation of the aforementioned primary vinylidene **3**.

Theoretical Study

Structural Analysis. The theoretical study started by searching equilibrium structures on the potential energy surface of the $[\text{CpRu}(\text{C}_2\text{H}_2)(\text{PH}_3)_2]^+$ (**A**) model system. We found three minima **1A**, **2A**, and **3A**, corresponding respectively, to the three X-ray characterized complexes, i.e., the η^2 -acetylene complex **1**, the alkynyl-hydride complex **2** and the η^1 -vinylidene complex **3**. The geometries of model complexes **1A**, **2A**, and **3A** were fully optimized without any symmetry constraints, and their natures as minima were confirmed by normal-mode analysis.

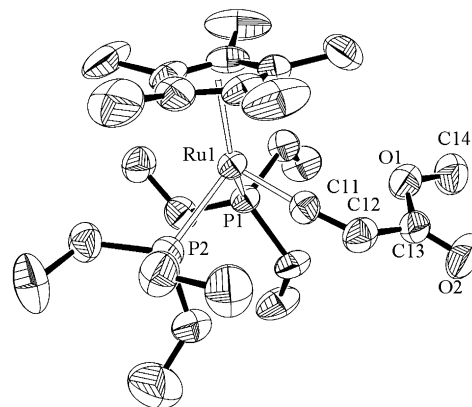


Figure 5. ORTEP drawing (50% thermal ellipsoids) of $[\text{Cp}^*\text{Ru}(\text{C}=\text{CHCOOMe})(\text{PEt}_3)_2]^+$ (**10**).

Table 3. Selected Bond Lengths (Å) and Angles (deg) for Compound **10** with Estimated Standard Deviations in Parentheses

bond distances (Å)		bond angles (deg)	
10			
Ru(1)P(1)	2.360(2)	P(1)Ru(1)P(2)	92.15(8)
Ru(1)P(2)	2.340(2)	P(1)Ru(1)C(11)	87.6(2)
Ru(1)C(11)	1.806(8)	P(2)Ru(1)C(11)	92.4(2)
C(11)C(12)	1.308(10)	Ru(1)C(11)C(12)	175.4(6)
C(12)C(13)	1.450(12)	C(11)C(12)C(13)	123.3(8)

The X-ray determined structure of compound **2** shows a transoid disposition of the alkynyl and hydride ligands with a $\text{C}_{\text{alkynyl}}-\text{Ru}-\text{H}_{\text{hydride}}$ angle of 131.3(16)°. The computed value of $\text{C}_{\text{alkynyl}}-\text{Ru}-\text{H}_{\text{hydride}}$ angle in complex **2A** is 129.2°, very close to the experimental one. Another alkynyl-hydride isomer is still conceivable, that with the alkynyl and hydride ligands in cisoid disposition. However, and despite the many efforts made, it has not been possible to find such alkynyl-hydride isomer. Instead, we located a stable minimum corresponding to a η^2 -(C,H) coordination of the acetylene moiety to the metal. The participation of such σ alkyne complex as intermediate in the alkyne-vinylidene isomerization has been suggested in several theoretical studies.^{2b,5a,b,6} It is noteworthy that in recent theoretical works on analogous d^6 half-sandwich systems, $[\text{CpRu}(\text{PH}_3)_2(\text{C}_2\text{HMe})]^+$ ^{7d} and $\text{CpMn}(\text{CO})_2(\text{C}_2\text{H}_2)$,^{2b} only the transoid alkynyl-hydride isomer was characterized as a minimum, with $\text{C}_{\text{alkynyl}}-\text{M}-\text{H}_{\text{hydride}}$ angles of 122.9° and 132.5°, respectively. Moreover, both studies found structures with $\text{C}_{\text{alkynyl}}-\text{M}-\text{H}_{\text{hydride}}$ angles of 68.0° and 78.4° respectively, corresponding to the transition states for the oxidative addition from the alkyne to the alkynyl-hydride isomer.

Relevant geometric features of the X-ray data are compared in Table 4 to the calculated results of the full ab initio model $[\text{CpRu}(\text{C}_2\text{H}_2)(\text{PH}_3)_2]^+$ (**A**), and the quantum mechanics/molecular mechanics (QM/MM) model $[\text{Cp}^*\text{Ru}(\text{C}_2\text{H}_2)(\text{PEt}_3)_2]^+$ (**B**). The calculated metal-carbon (Ru–C α) and carbon-carbon (C α –C β) distances in **1A**, **2A**, and **3A** (2.252, 2.252 and 1.247 Å, 2.048 and 1.219 Å, and 1.871 and 1.306 Å, respectively) agree well with the distances determined by X-ray diffraction (2.182(4), 2.180(5) and 1.220(7) Å for **1**, 2.034(4) and 1.150(6) Å for **2**, 1.835(8) and 1.296(11) Å for **3**), reflecting the change of bond orders in the different isomers. On the other hand, the computed values of the P–Ru–P angle (89.4°, 103.8°, and 90.5° for **1A**, **2A** and **3A**, respectively) are lower than those obtained from the X-ray diffraction analysis (93.67(4)°,

Table 4. Relevant Bond Lengths (Å) and Angles (deg) of the Calculated Structures of Simplified Model [CpRu(PH₃)₂(C₂H₂)]⁺ (**A**) and QM/MM Model [Cp*Ru(PEt₃)₂(C₂H₂)]⁺ (**B**) Compared to X-ray Structural Data

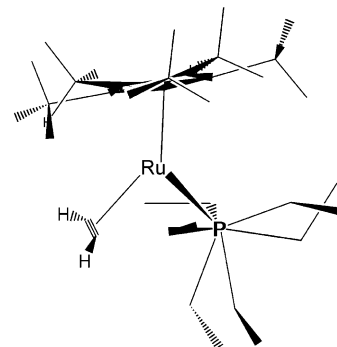
parameter	π -alkyne			alkynyl-hydride			vinylidene		
	1	1A	1B	2	2A	2B	3	3A	3B
	X-ray	full ab initio	QM/MM	X-ray	full ab initio	QM/MM	X-ray	full ab initio	QM/MM
Ru–C α	2.180(5)	2.252	2.252	2.034(4)	2.048	2.041	1.835(8)	1.871	1.863
C α –C β	1.220(7)	1.247	1.245	1.150(6)	1.219	1.219	1.296(11)	1.306	1.308
P–Ru–P	93.67(4)	89.4	94.1	107.20(4)	103.8	105.5	96.85(7)	90.5	96.2

107.20(4)°, and 96.85(7)° for **1**, **2** and **3**, respectively). The computed structure of complex **1A** shows an orthogonal arrangement of the acetylene unit with torsion angles Cp–Ru–Mp–C_{alkyne} (Cp, ring centroid; Mp, alkyne C≡C midpoint) of 90.0° and –90.0°, whereas in the X-ray structure of **1** the torsion angles are 69.3° and –110.7°.

It was described above that, in acetylene complex **1**, the rotational orientation of the acetylene unit relative to the [Cp*Ru(PEt₃)₂]⁺ moiety deviates from its ideal perpendicular arrangement. However, the optimization of compound [CpRu(PH₃)₂(HC≡CH)]⁺ (**1A**) revealed a preference for perpendicular disposition. To evaluate the energy cost of acetylene deviation we performed a partial optimization, forcing the torsion angles P–Ru–C_{alkyne}–C_{alkyne} to remain at the values of the crystal structure. The resulting structure was found only 0.7 kcal·mol^{–1} above the minimum **1A**. This value gives an estimation of the energy cost for acetylene distortion, indicating a very low energy cost for the rotation of the acetylene from its idealized position to that found in X-ray data. Furthermore, the computed energy barrier for rotation of acetylene unit around the metal fragment is not high, 8.2 kcal·mol^{–1}.

The lower values of P–Ru–P angles found for [CpRu(C₂H₂)(PH₃)₂]⁺ (**A**) indicate that the PH₃ model phosphine does not reproduce the steric hindrance induced by triethylphosphine ligands, suggesting that this missing effect could be responsible for discrepancies with experimental data in acetylene arrangement. To analyze acetylene distortion, hybrid quantum mechanics/molecular mechanics (QM/MM) with the IMOMM method¹⁸ were carried out on a more realistic system [Cp*Ru(C₂H₂)(PEt₃)₂]⁺ (**B**). The QM region was [CpRu(C₂H₂)(PH₃)₂]⁺, whereas the MM region included the methyl and ethyl substituents of Cp and phosphine, respectively. Note that this QM/MM method accounts only for the steric properties of the atoms included in the MM region. The inclusion of steric effects of bulky ligands is reflected on an increase of the computed P–Ru–P angle with respect to model **A** to values closer to the experimental ones (Table 4). Now, the computed torsion angles Cp–Ru–Mp–C_{alkyne} are 74.0° and –106.0°, reproducing the experimental observed acetylene distortion. Thus, the incorporation of the steric effects of bulky ligands distorts the rotational orientation of acetylene in **1B**, despite the electronic preference for the perpendicular arrangement found in **1A**.

These findings may seem surprising since the metal fragment [Cp*Ru(PEt₃)₂]⁺ possess in principle a symmetry molecular plane containing the Ru atom, the Cp centroid and bisecting the two phosphine ligands. However, a closer inspection of the structure **1B** revealed that the bulky substituents of the phosphine ligand are alternate (Scheme 4). This configuration breaks the

Scheme 4

symmetry at the metal center and induces a distortion of the acetylene unit in order to minimize the steric repulsion.

To further confirm our arguments we carried out additional pure quantum mechanics calculations on two additional model systems [Cp*Ru(C₂H₂)(PH₃)₂]⁺ (**C**), and [CpRu(C₂H₂)(PMe₃)₂]⁺ (**D**). In the case of alkyne complex **1C**, where the Cp ligand has been replaced by a Cp* but keeping the simple PH₃ phosphines, no acetylene distortion was observed. On the other hand, in complex **1D**, where the simple PH₃ phosphines were replaced by the bulkier PMe₃ phosphines but keeping the Cp model ligand, the rotational orientation of acetylene deviates from its ideal perpendicular disposition with torsion angles Cp–Ru–Mp–C_{alkyne} of 79.4° and –100.6°. Therefore, these results support the fact that the steric effect induced by the bulky phosphine substituents is responsible of the acetylene distortion.

Relative Energies of the Three Isomers. The calculated relative energies of the three C₂H₂ isomers for **A**, **B**, **C**, and **D** systems are summarized in Table 5. The vinylidene complex **3A** is found as the global energy minimum structure, being 8.6 and 28.5 kcal·mol^{–1} lower than the acetylene **1A** and alkynyl-hydride **2A** complexes, respectively. Thus, the alkynyl-hydride complex lays 19.9 kcal·mol^{–1} above the acetylene complex. Although predicting the vinylidene as the most stable isomer is alike the experimental results, the high destabilization of alkynyl-hydride with respect to the acetylene isomer does not seem to agree with experimental observations.

Our DFT methodology has been successfully tested in a previous study of alkyne-vinylidene isomerization on the coordination sphere of niobocene complexes.^{5a} The calculated relative energy for the free vinylidene with respect to acetylene at our computational level (41.8 kcal·mol^{–1}) reproduces previous theoretical¹⁹ and experimental results.²⁰ Furthermore, the result for F₄W system (alkyne isomer 8.1 kcal·mol^{–1} more stable than

(18) (a) Maseras, F.; Morokuma, K. *J. Comput. Chem.* **1995**, *16*, 1170. (b) Maseras, F. *Chem. Commun.* **2000**, 1821–1827.

(19) See, for example: (a) Gallo, M. M.; Hamilton, T. P.; Schaefer, H. F. *J. Am. Chem. Soc.* **1990**, *112*, 8714. (b) Petersson, G. A.; Tensfeldt, T. G.; Montgomery, J. A., Jr. *J. Am. Chem. Soc.* **1992**, *114*, 6133. (c) Jensen, J. H.; Morokuma, K.; Gordon, M. S. *J. Chem. Phys.* **1994**, *100*, 1981.

Table 5. Calculated Relative Energies of the Three C₂H₂ Isomers for **A**, **B**, **C** and **D** Systems. Energies in kcal·mol⁻¹

	CpRu(C ₂ H ₂) (PH ₃) ₂] ⁺	[Cp* ₂ Ru(C ₂ H ₂) (PEt ₃) ₂] ⁺	[Cp* ₂ Ru(C ₂ H ₂) (PEt ₃) ₂] ⁺	[[Cp* ₂ Ru(C ₂ H ₂) (PH ₃) ₂] ⁺	[CpRu(C ₂ H ₂) (PMe ₃) ₂] ⁺
isomer	QM (A)	QM/MM (B)	QM/QM/MM (B)	QM (C)	QM (D)
acetylene	+8.6	+15.7	+16.3	+8.2	+12.4
alkynyl-hydride	+28.5	+27.6	+19.6	+25.0	+23.1
vinylidene	0.0	0.0	0.0	0.0	0.0

vinylidene) is also in agreement with previously reported value at the CCSD(T)//DFT level (10.4 kcal·mol⁻¹).^{5b}

It is worth comparing the thermodynamics of the system with those reported in previous theoretical works for analogous d⁶ metal systems: Ru(II) [Cl₂Ru(PH₃)₂(C₂H₂)],^{7a} [CpRu(PH₃)₂(C₂HMe)]⁺,^{7d} Mn(I) [CpMn(CO)₂(C₂H₂)],^{2b} and Os(II) [CpOs-(PH₃)₂(C₂H₂)]⁺.^{8c} In all cases, the vinylidene isomer is predicted to be the most stable one, whereas the alkynyl-hydride isomer is the highest in energy. These thermodynamic trends are in the line with those computed for our model system [CpRu-(C₂H₂)(PH₃)₂]⁺ (**A**). In fact, it has been proposed^{7a,10d} that for d⁶ systems the oxidative addition of the alkyne to the alkynyl-hydride complexes is difficult since the metal changes from d⁶ to d⁴. However, this is not the case of the metal system under investigation, in which the acetylene complex **1** isomerizes spontaneously to the corresponding alkynyl-hydride complex **2**.

Up till now, theoretical studies have only been performed on simplified model systems. Here, we have carried out QM/MM calculations on the real system [Cp*₂Ru(C₂H₂)(PEt₃)₂]⁺ (**B**), because it seems that the simplified models do not account for the experimental complexity. The results show that the acetylene isomer **1B** and the alkynyl-hydride **2B** are respectively, 15.7 and 27.6 kcal·mol⁻¹ higher in energy than the vinylidene isomer **3B**. On going from model **A** to **B**, i.e., including the steric effects of ligand substituents, we observed that the acetylene isomer is destabilized with respect to the vinylidene in 7.1 kcal·mol⁻¹ (from 8.6 to 15.7 kcal·mol⁻¹), whereas the relative stability of the alkynyl-hydride isomer remains practically unchanged (from 28.5 to 27.6 kcal·mol⁻¹). This also implies a significant reduction of the energy difference between the acetylene and the alkynyl-hydride complexes, from 19.9 to 11.9 kcal·mol⁻¹.

During the last years the hybrid QM/MM methods have emerged as a powerful tool in the study of organometallic compounds. The IMOMM and related methods have been successfully applied to a range of problems such as homogeneous catalysis²¹ or structural issues associated with steric effects.²² However, in these methods the electronic contributions of the MM atoms are left out. To evaluate the electronic effects

of the ligands substituents in the relative stabilities of the three C₂H₂ isomers, we performed full ab initio energy calculations on the optimized QM/MM geometries of model [Cp*₂Ru(C₂H₂)-(PEt₃)₂]⁺ (**B**). Taking as the zero of energy the vinylidene species, the energies of the acetylene and the alkynyl-hydride isomers are +16.3 and +19.6 kcal·mol⁻¹, respectively. The comparison of the relative energies with those obtained in QM/MM calculation on **B**, shows a substantial energy lowering of the alkynyl-hydride isomer (8.0 kcal·mol⁻¹, from 27.6 to 19.6 kcal·mol⁻¹) and small energy variation of the acetylene isomer (from 15.7 to 16.3 kcal·mol⁻¹), in marked contrast with that found on going from model **A** to **B**. The most striking result is that relative energies of the acetylene and alkynyl-hydride isomers became very similar (3.3 kcal·mol⁻¹), in better agreement with the experimental results because both isomers could be prepared. The energy differences between the two forms that were found are within the limits of accuracy of the modeling and the methodology employed, but a definitive answer with regard to which is the most stable species cannot be established. To the best of our knowledge this is the first time that QM/MM methods have been used this way, i.e., combined with full ab initio energy calculation. The success in reproducing experimental trends suggests that this procedure could be useful when the electronic ligand effects are important to model experimental complexity, expanding the range of applications of these methods.

In summary, the sequential refinement of the model system has allowed separating, identifying and evaluating different contributions of the ligands to the thermodynamics of the system. The sequence is schematically depicted in Figure 6. First, upon introduction of steric effects of bulky ligand substituents, is observed a relative destabilization of the alkyne form, while the relative energy of alkynyl-hydride complex remains almost unchanged. Second, recovering the electronic effects of the donor substituents causes a stabilization of the alkynyl-hydride form with respect to the alkyne and the vinylidene. The combination of these two effects makes alkyne and alkynyl-hydride complexes to be very close in energy, allowing the isolation of the unusual ruthenium alkynyl-hydride complex.

To analyze in more detail the contributions of the different ligands to thermodynamics, pure quantum mechanics calculations have been carried out on [(C₅Me₅)Ru(C₂H₂)(PH₃)₂]⁺ (**C**) and [CpRu(C₂H₂)(PMe₃)₂]⁺ (**D**) model systems. The replacement of the Cp ligand (model **A**) by the better π donor Cp* ligand (model **C**) stabilizes the alkynyl-hydride isomer with respect to vinylidene in about 4 kcal·mol⁻¹, whereas the relative energy of the acetylene isomer remains very similar (from 8.6 to 8.2 kcal·mol⁻¹). Moreover, the presence of the bulkier and

- (20) (a) Ervin, K. M.; Ho, J.; Lineberger, W. C. *J. Chem. Phys.* **1989**, *91*, 5974. (b) Ervin, K. M.; Gronert, S.; Barlow, S. E.; Gilles, M. K.; Harrison, A. G.; Bierbaum, V. M.; De Puy, C. H.; Lineberger, W. C.; Ellison, G. B. *J. Am. Chem. Soc.* **1990**, *112*, 5750. (c) Chen, Y.; Jonas, D. M.; Hamilton, C. E.; Green, P. G.; Kinsey, J. L.; Field, R. W. *Ber. Bunsen-Ges. Phys. Chem.* **1988**, *92*, 329. (d) Chen, Y.; Jonas, D. M.; Kinsey, J. L.; Field, R. W. *J. Chem. Phys.* **1989**, *91*, 3976.
- (21) For some recent references, see: (a) Ujaque, G.; Maseras, F.; Lledós, A. *J. Am. Chem. Soc.* **1999**, *121*, 1317. (b) Vázquez, J.; Pericàs, M. A.; Maseras, F.; Lledós, A. *J. Org. Chem.* **2000**, *65*, 7303. (c) Carbó, J. J.; Maseras, F.; Bo, C.; van Leeuwen, P. W. N. M. *J. Am. Chem. Soc.* **2001**, *123*, 7630–7637. (d) Feldgus, S.; Landis, C. R. *J. Am. Chem. Soc.* **2000**, *122*, 12714. (e) Feldgus, S.; Landis, C. R. *Organometallics* **2001**, *20*, 2374. (f) Goldfuss, B.; Steigelmann, M.; Khan, S. I.; Houk, K. N. *J. Org. Chem.* **2000**, *65*, 77. (g) Cavallo, L.; Solà, M. *J. Am. Chem. Soc.* **2001**, *123*, 12 294. (h) Milano, G.; Guerra, G.; Pellecchia, C.; Cavallo, L. *Organometallics* **2000**, *19*, 1343. (i) Musaev, D. G.; Froese, R. D. J.; Morokuma, K. *Organometallics* **1998**, *17*, 1850.

- (22) (a) Barea, G.; Lledós, A.; Maseras, F.; Jean, Y. *Inorg. Chem.* **1998**, *37*, 3321. (b) Ujaque, G.; Cooper, A. C.; Maseras, F.; Eisenstein, O.; Caulton, K. G. *J. Am. Chem. Soc.* **1998**, *120*, 361.

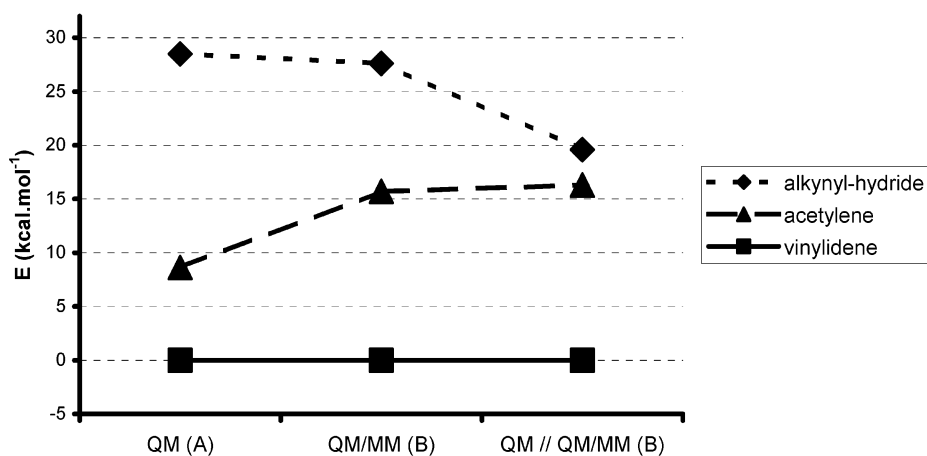
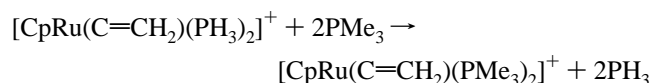
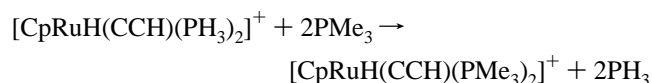
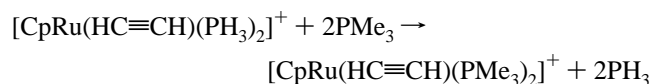


Figure 6. Schematic representation of the evolution of the relative energies of the three C_2H_2 isomers upon successive introduction of steric effects (QM/MM (A)) and electronic effects (QM//QM/MM (B)).

more basic PMe_3 phosphines in model **D** instead of the PH_3 used in model **A** led to a higher destabilization of the alkyne species (from 8.6 to 12.4 $\text{kcal}\cdot\text{mol}^{-1}$) and to the stabilization of the alkynyl-hydride species (from 28.5 to 23.1 $\text{kcal}\cdot\text{mol}^{-1}$). The destabilization of the alkyne isomer is due to the greater steric hindrance of PMe_3 phosphines, whereas the stabilization of alkynyl-hydride isomer is due to the higher basicity with respect to PH_3 phosphine. Up until now, the discussion has been done on the basis of the relative energies of the different isomers with respect to vinylidene species. To gain insight into the overall energetics of the phosphine exchange we make use of ligand-transfer reactions



This kind of scheme provides a measure of the stability change caused by the replacement of phosphine ligands for a given isomer. The energy change for the ligand-transfer reaction of acetylene, alkynyl-hydride and vinylidene isomers are, respectively, +1.6, -8.0, and -2.4 $\text{kcal}\cdot\text{mol}^{-1}$. For alkynyl-hydride and vinylidene the reaction is exothermic, indicating the preference for basic phosphines, especially in the case of alkynyl-hydride. On the other hand, for acetylene isomer the reaction is endothermic, indicating that the use of bulkier phosphines destabilizes the complex. Finally, we can conclude that bulky phosphine ligands work against the most steric hindered isomer, the acetylene, whereas the use of basic phosphines and σ donor ligands makes more electron rich the metal center, favoring the obtaining of the alkynyl-hydride isomer.

It is clear from our results, particularly from the energies of the ligand exchange reactions that the hydride-alkynyl isomer is especially sensitive to back-donation effects. Back-bonding could be slightly underestimated in DFT calculations, and the hydrido-alkynyl isomer could become even more competitive

with the acetylene isomer using high-level computational methods (as CCSD(T)) able to represent better back-bonding. Unfortunately such calculations are not feasible at the present time, and a definitive answer about which is the most stable species cannot be done at this time.

Conclusions

In the present paper, we have reported new experimental data and theoretical support on the alkyne/vinylidene isomerization, which has been during the past decades a permanent subject of research on the field of the organometallic chemistry. The X-ray structures of the three isomers involved in the activation of acetylene by a particular transition metal complex have been determined for the first time. The isolation and structural characterization of the three isomers provides a sound experimental proof of the existence and accessibility of such species. In general, π -alkyne, alkynyl-hydride, and vinylidene isomers are species mutually exclusive due to their opposed thermodynamic stabilities, but they have been frequently proposed as the necessary intermediates in the way to vinylidenes. Moreover, in the chemistry of ruthenium the isomerization to vinylidene via 1,2-H shift from the π -alkyne has an experimental and theoretical support as the most feasible explanation for the tautomerization process. The alternative pathway via alkynyl-hydride intermediates has been proven to be accessible by $[\text{Cp}^*\text{Ru}(\text{P})_2]^+$ systems ($\text{P}_2 = \text{dippe}, 2 \text{PEt}_3$), which exhibit a remarkable different behavior. Additionally, we have used the structural data obtained from the X-ray diffraction analysis as the starting point to carry out theoretical studies on this system. These studies have separated and identified the reasons that explain the observed behavior on the basis of the electronic and steric effects induced by the auxiliary ligands. On the other hand, the ability of theoretical methods to predict molecular features has been tested against a number of experimental facts observed in our particular system. This comparison has led to a sequential refinement of the model system, allowing to separate, identify, and evaluate the different contributions to the thermodynamics of the system. Thus, the bulkiness of phosphine ligand induces alkyne distortion and relative destabilization of alkyne isomer, whereas the donor capabilities of the auxiliary ligands are responsible of relative stabilization of vinylidene isomer. The combination of these two effects is behind the reason the three C_2H_2 isomers have been isolated in this particular system.

Furthermore, we proved that small changes in auxiliary ligands have a dramatic influence in the relative energies of the different isomers, so caution should be taken when modeling these systems. The novel application of QM/MM methods combined with full ab initio energy calculation, and the success in reproducing experimental trends, allow to propose the potential utility of this procedure in situations where a particular configuration of ligands around a metal induces unusual properties or exhibits a comparatively different behavior.

Experimental Section

All synthetic operations were performed under a dry dinitrogen or argon atmosphere by following conventional Schlenk techniques. Tetrahydrofuran, diethyl ether and petroleum ether (boiling point range, 40–60 °C) were distilled from the appropriate drying agents. All solvents were deoxygenated immediately before use. IR spectra were recorded in Nujol mulls on a Perkin-Elmer FTIR Spectrum 1000 spectrophotometer. NMR spectra were taken on a Varian Unity 400 MHz or Varian Gemini 200 MHz equipment. Chemical shifts are given in parts per million from SiMe₄ (¹H and ¹³C{¹H}) or 85% H₃PO₄ (³¹P-{¹H}). NMR data of the [BPh₄]⁻ ion appeared in the appropriate shift ranges for cationic compounds isolated as its salts and are omitted for clarity. Microanalysis was performed by the Serveis Científic-Tècnics, Universitat de Barcelona.

Preparation of the Alkyne Complex [Cp*Ru(η^2 -HC≡CH)(PEt₃)₂][BPh₄] (1). Acetylene gas was bubbled through a solution of NaBPh₄ (194 mg, 1.2 mmol) in 10 mL of methanol. The addition of [Cp*RuCl(PEt₃)₂] (508 mg, 1 mmol) caused the immediate precipitation of a yellow solid, which was filtered, washed with ethanol and petroleum ether, dried under vacuum and stored at -20 °C. Yield: 695 mg (85%). This compound was recrystallized from an ethanol/acetone mixture (3:1) at -20 °C, yielding a mixture of yellow crystals corresponding to **1** (minor) and **2** (major). Microanalysis and selected spectral data are as follows.

(1). Anal. Calcd for C₄₈H₆₇BP₂Ru: C, 70.5; H, 8.26. Found: C, 70.5; H, 8.25. IR (Nujol): $\nu(\eta^2\text{-C}\equiv\text{C})$ 1732, $\nu(\text{BPh}_4)$ 1580 cm⁻¹. ¹H NMR (400 MHz, CDCl₃, 253 K): δ 1.07 (m, 18 H, PCH₂CH₃), 1.53 (s, 15 H, C₅(CH₃)₅), 1.69 (m, 12 H, PCH₂CH₃), 4.38 (t, 2 H, ³J_{HP} = 6.3 Hz, C₂H₂). ³¹P{¹H} NMR (161.9 MHz, CDCl₃, 253 K): δ 23.82 (s). ¹³C-{¹H} NMR (100.6 MHz, CDCl₃, 253 K): δ 9.11 (s, PCH₂CH₃), 10.21 (s, C₅(CH₃)₅), 19.83 (vt, ^{1,3}J_{CP} = 13.7 Hz, PCH₂CH₃), 66.14 (t, ²J_{CP} = 3.5 Hz, C₂H₂), 96.90 (s, C₅(CH₃)₅).

Preparation of the Alkynyl-Hydride Complex [Cp*Ru(H)(C≡CH)(PEt₃)₂][BPh₄] (2). A solution of complex **1** (150 mg, 0.18 mmol) in 5 mL of CH₂Cl₂ was kept at -20 °C for 72 h, undergoing spontaneous and irreversible isomerization to the alkynyl-hydride isomer **2**. The solvent was removed under vacuum and a pale yellow solid was obtained in quantitative yield. This compound must be stored below room temperature to prevent isomerization to vinylidene. Suitable crystals for XRD analysis were obtained from the recrystallization of the parent alkyne complex **1**. Microanalysis and selected spectral data are as follows.

(2). Anal. Calcd for C₄₈H₆₇BP₂Ru: C, 70.5; H, 8.26. Found: C, 70.5; H, 8.25. IR (Nujol): $\nu(\text{C}\equiv\text{C})$ 1965, $\nu(\text{Ru-H})$ 1935, $\nu(\text{BPh}_4)$ 1580 cm⁻¹. ¹H NMR (400 MHz, CDCl₃, 278 K): δ -9.27 (t, 1 H, ²J_{HP} = 29.5 Hz, Ru-H), 1.11 (m, 18 H, PCH₂CH₃), 1.70 (s, 15 H, C₅(CH₃)₅), 1.82 (m, 12 H, PCH₂CH₃), 2.09 (t, 1 H, ⁴J_{HP} = 2.7 Hz, C≡CH). ³¹P{¹H} NMR (161.9 MHz, CDCl₃, 278 K): δ 37.7 (s). ¹³C{¹H} NMR (100.6 MHz, CDCl₃, 278 K): δ 8.90 (vt, ^{3,5}J_{HP} = 3.0 Hz, PCH₂CH₃), 10.07 (s, C₅(CH₃)₅), 20.14 (m, PCH₂CH₃), 93.09 (t, ²J_{CP} = 29 Hz, C α), 101.4 (s, C₅(CH₃)₅), 102.1 (s, C β).

Preparation of the Vinylidene Complex [Cp*Ru(=C=CH₂)(PEt₃)₂][X] (3). **Method A.** Complex **3** was initially obtained as BPh₄ salt by the spontaneous isomerization of the ethynyl-hydride precursor

2 in a CH₂Cl₂ solution, which takes place at temperatures over 10 °C. This procedure requires a careful temperature control to avoid side-reactions, which occur above 20 °C. In these conditions, although the yielding is almost quantitative, the process is rather slow.

Method B. A solution of **1** (300 mg, 0.36 mmol) in THF (5 mL) was treated with an excess of ^tBuOK (114 mg, 95%, 1.0 mmol). The mixture was stirred for 15 min at room temperature, and then taken to dryness. The residue extracted with petroleum ether (2 × 5 mL). The yellow solution was then filtered through diatomaceous earth and the solvent removed under vacuum, affording a yellow microcrystalline solid corresponding to the neutral alkynyl complex **4**. Microanalysis and selected spectral data for complex **4** are reported below. A solution of **4** in Et₂O (3 mL) was cooled in an ethanol/liquid N₂ bath, and treated with 10 μ L of HBF₄ (85% solution of HBF₄·Et₂O). An orange solid was immediately formed. The bath was removed and the mixture was allowed to reach room temperature. The solid was separated by decantation, washed twice with Et₂O (3 mL) and dried in vacuo, corresponding to the vinylidene complex **3** as a BF₄ salt. Yield: 144 mg (68.3% from **1**).

Method C. A solution of [Cp*RuCl(PEt₃)₂] (508 mg, 1 mmol) and trimethylsilylacetylene (170 μ L, 1.2 mmol) in MeOH (10 mL) was stirred for 24 h at room temperature. Addition of NaBPh₄ (194 mg, 1.2 mmol) caused the immediate precipitation of an orange solid, which was separated by filtration and washed with EtOH and petroleum ether. Recrystallization from CH₂Cl₂/petroleum ether (1:2) yielded orange crystals suitable for X-ray structural analysis. Yield: 736 mg (90%).

(3). Anal. Calcd for C₄₈H₆₇BP₂Ru: C, 70.5; H, 8.26. Found: C, 70.5; H, 8.26. IR (Nujol): $\nu(\text{C}\equiv\text{C})$ 1611, $\nu(\text{BPh}_4)$ 1580 cm⁻¹. ¹H NMR (400 MHz, CDCl₃, 298 K): δ 1.00 (m, 18 H, PCH₂CH₃), 1.78 (s, C₅(CH₃)₅), 1.62 and 1.84 (m, 12 H, PCH₂CH₃), 3.57 (t, 2 H, ⁴J_{HP} = 1.8 Hz, C≡CH₂). ³¹P{¹H} NMR (161.9 MHz, CDCl₃, 298 K): δ 31.7 (s). ¹³C-{¹H} NMR (100.6 MHz, CDCl₃, 298 K): δ 8.86 (s, PCH₂CH₃), 10.84 (s, C₅(CH₃)₅), 21.19 (m, PCH₂CH₃), 93.77 (s, C₅(CH₃)₅), 102.9 (s, C β), 345.9 (t, ²J_{CP} = 21.5 Hz, C α).

Preparation of the Neutral Ethynyl Complex [Cp*Ru(C≡CH)(PEt₃)₂] (4). This compound has been obtained and characterized in the two steps synthesis of the vinylidene complex **3**, as it was described above. Yield: 167 mg (93%). Microanalysis and selected spectral data are as follows.

(4). Anal. Calcd for C₂₄H₄₆P₂Ru: C, 57.9; H, 9.32. Found: C, 57.8; H, 9.30. IR (Nujol): $\nu(\text{C}\equiv\text{C})$ 1942 cm⁻¹. ¹H NMR (400 MHz, C₆D₆, 298 K): δ 1.02 (m, 18 H, PCH₂CH₃), 1.74 (s, 15 H, C₅(CH₃)₅), 1.57 and 1.81 (m, 12 H, PCH₂CH₃), 2.05 (t, 1 H, ⁴J_{HP} = 2.2 Hz, C≡CH). ³¹P{¹H} NMR (161.9 MHz, C₆D₆, 298 K): δ 32.4 (s). ¹³C{¹H} NMR (100.6 MHz, C₆D₆, 298 K): δ 9.00 (s, PCH₂CH₃), 11.25 (s, C₅(CH₃)₅), 22.00 (vt, ^{1,3}J_{CP} = 11.5 Hz, PCH₂CH₃), 91.29 (s, C β), 92.22 (s, C₅(CH₃)₅), 108.9 (t, ²J_{CP} = 25.9 Hz, C α).

Preparation of the Alkynyl-Hydride Complexes [Cp*Ru(H)(C≡CR)(PEt₃)₂][BPh₄] (R = SiMe₃ (5), Ph (6), COOMe (7), ^tBu (8)). To a solution of the corresponding alkyne (0.40 mmol) and NaBPh₄ (81 mg, 0.50 mmol) in 10 mL of MeOH at 0 °C (ice bath), were added 127 mg (0.25 mmol) of [Cp*RuCl(PEt₃)₂]. The bath was removed and the mixture allowed to warm until a white microcrystalline solid precipitated. This solid was immediately filtered, washed with cold ethanol and petroleum ether, and dried under vacuum. Complexes **5**, **6**, and **8** were stored at 0 °C to prevent the isomerization to vinylidene.

(5). Yield: 175 mg (79%). Anal. Calcd for C₅₁H₇₅BP₂RuSi: C, 68.8; H, 8.49. Found: C, 69.0; H, 8.50. IR (Nujol): $\nu(\text{C}\equiv\text{C})$ 2039, $\nu(\text{Ru-H})$ 2142 cm⁻¹. ¹H NMR (400 MHz, CDCl₃, 253 K): δ -9.20 (t, 1 H, ²J_{HP} = 27.0 Hz, Ru-H), 0.18 (s, 9 H, Si(CH₃)₃), 1.08 (m, 18 H, PCH₂CH₃), 1.75 (s, 15 H, C₅(CH₃)₅), 1.81 (m, 12 H, PCH₂CH₃). ³¹P{¹H} NMR (161.9 MHz, CDCl₃, 253 K): δ 37.6 (s). ¹³C{¹H} NMR (100.6 MHz, CDCl₃, 253 K): δ 0.82 (s, Si(CH₃)₃), 8.95 (s, PCH₂CH₃), 10.00 (s, C₅(CH₃)₅), 20.02 (m, PCH₂CH₃), 101.7 (s, C₅(CH₃)₅), 106.1 (s, C α), 121.9 (s, C β).

Table 6. Summary of Crystallographic Data for Compounds **1–3** and **10**

compd	1	2	3	10
formula	C ₄₈ H ₆₇ BP ₂ Ru	C ₄₈ H ₆₇ BP ₂ Ru	C ₄₈ H ₆₇ BP ₂ Ru	C ₅₀ H ₆₉ BO ₂ P ₂ Ru
FW	817.84	817.84	817.84	875.87
<i>T</i> (K)	183(2)	183(2)	293(2)	293(2)
crystal color	yellow, prism	yellow, prism	yellow, plate	yellow, prism
crystal system	monoclinic	orthorhombic	orthorhombic	monoclinic
space group	P2(1)/c	P2(1)2(1)2(1)	P2(1)2(1)2(1)	P2(1)/n
cell parameters	<i>a</i> = 10.424(3) Å <i>b</i> = 21.503(6) Å <i>c</i> = 19.484(5) Å $\alpha = \gamma = 90^\circ$ $\beta = 94.67(1)^\circ$	<i>a</i> = 13.604(2) Å <i>b</i> = 16.518(3) Å <i>c</i> = 19.219(3) Å $\alpha = \beta = \gamma = 90^\circ$	<i>a</i> = 13.5677(7) Å <i>b</i> = 17.2811(8) Å <i>c</i> = 19.0256(9) Å $\alpha = \beta = \gamma = 90^\circ$	<i>a</i> = 16.367(3) Å <i>b</i> = 16.006(5) Å <i>c</i> = 17.669(3) Å $\alpha = \gamma = 90^\circ$ $\beta = 95.13(2)^\circ$
<i>Z</i>	4	4	4	4
final R1, ^a wR2 ^b values (<i>I</i> > 2σI)	0.0477, 0.1211	0.0432, 0.1046	0.0640, 0.1314	0.0586, 0.1529
final R1, ^a wR2 ^b values (all data)	0.0635, 0.1325	0.0520, 0.1115	0.0678, 0.1333	0.1216, 0.1806
GOF	1.070	1.091	1.034	1.081

$$^a R1 = \sum\{[F_o] - [F_c]\} / \sum[F_o], \quad ^b wR2 = [\sum\{w(F_o^2 - F_c^2)^2\} / \sum\{w(F_o^2)^2\}]^{1/2}.$$

(6). Yield: 185 mg (83%). Anal. Calcd for C₅₄H₇₁BP₂Ru: C, 72.6; H, 8.01. Found: C, 72.8; H, 7.99. IR (Nujol): $\nu(\text{C}\equiv\text{C})$ 2105, $\nu(\text{Ru}-\text{H})$ 2016, $\nu(\text{Ph})$ 1592 cm⁻¹. ¹H NMR (400 MHz, CDCl₃, 273 K): δ -9.17 (t, 1 H, ²*J*_{HP} = 29.6 Hz, Ru-H), 1.12 (m, 18 H, PCH₂CH₃), 1.71 (s, 15 H, C₅(CH₃)₅), 1.83 (m, 12 H, PCH₂CH₃), 7.20 and 7.26 (m, 5 H, C₆H₅). ³¹P{¹H} NMR (161.9 MHz, CDCl₃, 273 K): δ 37.55 (s). ¹³C{¹H} NMR (100.6 MHz, CDCl₃, 273 K): 8.80 (s, PCH₂CH₃), 10.17 (s, C₅(CH₃)₅), 20.18 (m, PCH₂CH₃), 104.0 (t, ²*J*_{CP} = 30 Hz, Cα), 102.7 (s, C₅(CH₃)₅), 112.0 (s, Cβ), 124.4, 126.8, 127.0, and 143.2 (s, C₆H₅).

(7). Yield: 193 mg (88%). Anal. Calcd for C₅₀H₆₉BO₂P₂Ru: C, 68.6; H, 7.94. Found: C, 69.0; H, 7.93. IR (Nujol): $\nu(\text{C}\equiv\text{C})$ 2109, $\nu(\text{Ru}-\text{H})$ 2013, $\nu(\text{CO})$ 1693 cm⁻¹. ¹H NMR (400 MHz, CDCl₃, 273 K): δ -9.02 (t, 1 H, ²*J*_{HP} = 27.5 Hz, Ru-H), 1.10 (m, 18 H, PCH₂CH₃), 1.65 (s, 15 H, C₅(CH₃)₅), 1.77 (m, 12 H, PCH₂CH₃), 3.67 (s, COOCH₃). ³¹P{¹H} NMR (161.9 MHz, CDCl₃, 273 K): δ 37.54 (s). ¹³C{¹H} NMR (100.6 MHz, CDCl₃, 273 K): δ 8.75 (s, PCH₂CH₃), 10.06 (s, C₅(CH₃)₅), 20.18 (m, PCH₂CH₃), 52.07 (s, COOCH₃), 102.4 (s, C₅(CH₃)₅), 108.8 (t, ³*J*_{CP} = 4.1 Hz, Cβ), 112.2 (t, ²*J*_{CP} = 28.8 Hz, Cα), 183.4 (s, COOCH₃).

(8). This compound is obtained as a minor product besides the vinylidene isomer **11**, and only some of the spectral data have been identified: IR (Nujol): $\nu(\text{C}\equiv\text{C})$ 2143, $\nu(\text{Ru}-\text{H})$ 2042 cm⁻¹. ¹H NMR (400 MHz, CDCl₃, 273 K): -9.43 (t, 1 H, ²*J*_{HP} = 30.7 Hz, Ru-H). ³¹P{¹H} NMR (161.9 MHz, CDCl₃, 273 K): 36.73 (s).

Preparation of the Vinylidene Complexes [Cp*₂Ru(=C=CHR)-(PEt₃)₂][BPh₄] (R = Ph (9), COOMe (10), Bu(11)). 127 mg (0.25 mmol) of [Cp*₂RuCl(PEt₃)₂] were dissolved in 10 mL of MeOH. An excess of the corresponding 1-alkyne (0.40 mmol) was added and the solution was stirred for 6 h. NaBPh₄ (81 mg, 0.50 mmol) was added and an orange solid precipitated immediately. This solid was filtered, washed with EtOH and petroleum ether and dried under vacuum. Recrystallization of compound **10** from an acetone/ethanol solution (1:4), gave orange crystals suitable for X-ray structural analysis.

(9). Yield: 179 mg (80%). Anal. Calcd for C₅₄H₇₁BP₂Ru: C, 72.6; H, 8.01. Found: C, 72.8; H, 7.99. IR (Nujol): $\nu(\text{C}\equiv\text{C})$ 1621, $\nu(\text{Ph})$ 1592 cm⁻¹. ¹H NMR (400 MHz, CDCl₃, 298 K): δ 1.01 (m, 18 H, PCH₂CH₃), 1.79 (s, 15 H, C₅(CH₃)₅), 1.71 and 1.83 (m, 12 H, PCH₂CH₃), 5.12 (s, =C=CH), 7.12 and 7.27 (m, 5 H, C₆H₅). ³¹P{¹H} NMR (161.9 MHz, CDCl₃, 298 K): δ 27.84 (s). ¹³C{¹H} NMR (100.6 MHz, CDCl₃, 298 K): δ 13.41 (s, PCH₂CH₃), 11.45 (s, C₅(CH₃)₅), 22.84 (vt, ^{1,3}*J*_{CP} = 13.8 Hz, PCH₂CH₃), 102.5 (s, C₅(CH₃)₅), 113.4 (s, Cβ), 124.7, 127.0 and 145.3 (s, C₆H₅), 342.8 (t, ²*J*_{CP} = 19.0 Hz, Cα).

(10). Yield: 191 mg (87%). Anal. Calcd for C₅₀H₆₉BO₂P₂Ru: C, 68.6; H, 7.94. Found: C, 69.0; H, 7.93. IR (Nujol): $\nu(\text{C}\equiv\text{C})$ and $\nu(\text{CO})$ 1694 cm⁻¹. ¹H NMR (400 MHz, CDCl₃, 298 K): δ 1.01 and 1.17 (m, 18 H, PCH₂CH₃), 1.74 (s, 15 H, C₅(CH₃)₅), 1.71 and 1.83 (m, 12 H, PCH₂CH₃), 3.65 (s, COOCH₃), 4.70 (s, =C=CH). ³¹P{¹H} NMR (161.9

MHz, CDCl₃, 298 K): δ 28.45 (s). ¹³C{¹H} NMR (100.6 MHz, CDCl₃, 298 K): 8.81 (s, PCH₂CH₃), 10.79 (s, C₅(CH₃)₅), 20.60 (m, PCH₂CH₃), 51.47 (s, COOCH₃), 104.5 (s, C₅(CH₃)₅), 107.6 (s, Cβ), 165.6 (s, COOCH₃), 343.4 (t, ²*J*_{CP} = 15.0 Hz, Cα).

(11). Yield: 186 mg (85%). Anal. Calcd for C₅₂H₇₅BP₂Ru: C, 71.5; H, 8.65. Found: C, 71.8; H, 8.60. IR (Nujol): $\nu(\text{C}\equiv\text{C})$ 1666 cm⁻¹. ¹H NMR (400 MHz, CDCl₃, 298 K): δ 1.03 (m, 18 H, PCH₂CH₃), 1.12 (s, 9 H, C(CH₃)₃), 1.74 (s, 15 H, C₅(CH₃)₅), 1.69 and 1.82 (m, 12 H, PCH₂CH₃), 3.72 (s, =C=CH). ³¹P{¹H} NMR (161.9 MHz, CDCl₃, 298 K): δ 27.94 (s). ¹³C{¹H} NMR (100.6 MHz, CDCl₃, 298 K): δ 9.21 (s, C(CH₃)₃), 10.17 (s, PCH₂CH₃), 11.03 (s, C₅(CH₃)₅), 21.06 (m, PCH₂CH₃), 32.05 (s, C(CH₃)₃), 102.3 (s, C₅(CH₃)₅), 106.4 (s, Cβ), 347.1 (t, ²*J*_{CP} = 14.7 Hz, Cα).

X-ray Structure Determinations. Suitable crystals of compounds **1–3** and **10** were used for X-ray crystal structure analysis. Crystal data and experimental details are given in Table 6. Further details are given in the Supporting Information. X-ray data of **1** and **2** were collected on a Bruker AXS Smart CCD area detector diffractometer (graphite monochromated MoKα radiation, $\lambda = 0.71073$ Å, 0.3° ω -scan frames covering complete spheres of the reciprocal space), at the Institute of Chemical Technologies and Analytics, Vienna University of Technology. X-ray data of **3** were collected on a Bruker Smart Apex CCD area detector diffractometer (graphite-monochromated MoKα radiation, $\lambda = 0.71073$ Å, 0.3° ω -scan frames covering hemispheres of the reciprocal space). X-ray data of **10** were collected on a MSC-Rigaku AFC6S four-circle diffractometer (graphite-monochromated MoKα radiation, $\lambda = 0.71073$ Å, $\omega/2\theta$ scan method). Crystals **3** and **10** were measured at the Servicio Central de Ciencia y Tecnología de la Universidad de Cádiz.

In all the cases, corrections for Lorentz and polarization effects, for crystal decay, and for absorption were applied. All structures were solved using the program SHELXS97.²³ Structure refinements on *F*² were carried out with the program SHELXL97.²⁴ For compounds **1**, **3**, and **10**, all non-hydrogen atoms were anisotropically refined. Hydrogen atoms were refined in idealized positions riding with the atoms to which they were bonded. For compound **2**, two significant residual electron densities, labeled Ru(1') and P(2'), near Ru and P(2) were included in the refinement allowing to vary *x*, *y*, *z*, population and *U*_{iso} parameters. They are considered result of the presence of some 5% of the other isomer dihapto-alkyne. All other non-hydrogen atoms were anisotropically refined. Hydride hydrogen H(1) was refined unrestrained in *x*, *y*, *z*, and *U*_{iso}. All other hydrogen atoms were refined in idealized positions riding with the atoms to which they were bonded.

(23) Sheldrick, G. M. *SHELXS97, Program for Crystal Structure Solution*; University of Göttingen: Göttingen, Germany, 1997.

(24) Sheldrick, G. M. *SHELXL97, Program for Crystal Structure Refinement*; University of Göttingen, Göttingen: Germany, 1997.

Computational Details. Pure quantum mechanics calculations on [CpRu(C₂H₂)(PH₃)₂]⁺ (**A**), [Cp*Ru(C₂H₂)(PH₃)₂]⁺ (**C**) and [CpRu(C₂H₂)(PMe₃)₂]⁺ (**D**) model systems were performed with the GAUSSIAN 98 series of programs²⁵ within the framework of the Density Functional Theory (DFT)²⁶ using the B3LYP functional.²⁷ A quasi-relativistic effective core potential operator was used to represent the 28 innermost electrons of the Ru atom, as well as the 10 innermost electrons of the P atom.²⁸ The basis set for Ru and P atoms was that associated with the pseudopotential,²⁸ with a standard double- ξ LANL2DZ contraction,²⁵ and in the case of P was supplemented by a d shell.²⁹

The 6-31G(d,p) basis set was used for the C₂H₂ unit and the C atoms directly attached to the metal, whereas the 6-31G basis set was used for the other carbon and hydrogen atoms.³⁰ Geometry optimizations were carried out without any symmetry restrictions and all stationary points were optimized with analytical first derivatives. In the case of model complex **A**, the local minima corresponding to the three C₂H₂ isomers were identified by the absence of negative eigenvalues in the vibrational frequency analysis. The saddle point corresponding to

acetylene rotation in **1A** was located by means of approximate Hessians and synchronous transit-guided quasi-Newtonian methods.³¹

Hybrid QM/MM calculations with the IMOMM method¹⁸ were carried out on [Cp*Ru(C₂H₂)(PEt₃)₂]⁺ (**B**) real system with a program built from modified versions of the two standard programs GAUSSIAN 98²³ for quantum mechanics part and MM3(92)³² for the molecular mechanics part. The QM region was [(C₅H₅)Ru(C₂H₂)(PH₃)₂]⁺, whereas the methyl and ethyl substituents of the cyclopentadienyl and phosphine ligands were in the MM region. The quantum mechanics calculations were done with the use of the same method and basis set described above for the pure quantum mechanics calculations. Molecular mechanics calculations used the MM3(92) force field.³² Default parameters were used when available otherwise those of similar atoms replaced the missing ones. The van der Waals parameters for the Ru atom were taken from the UFF force field,³³ and torsional contributions involving dihedral angles with the metal atom in terminal position were set to zero. All the geometrical parameters were optimized except for the P–H (1.42 Å) and C(Cp)–H (1.101 Å) bond distances in the QM part of IMOMM and the P–C(sp³) (1.843 Å) and C(Cp)–C(sp³) (1.499 Å) distances in the MM part of IMOMM.

Acknowledgment. We wish to thank the Ministerio de Ciencia y Tecnología of Spain (DGI, Project BQU2001-4026 and BQU2002-04110-CO2-02) and Junta de Andalucía (PAI-FQM 0188) for financial support. We also thank Johnson Matthey plc for including us in their precious metal loan scheme.

Supporting Information Available: Tables of X-ray structural data, including data collection parameters, positional and thermal parameters, and bond distances and angles for complexes **1**, **2**, **3**, and **10**. Geometries of the calculated structures for the three isomers in the **A**, **B**, **C**, and **D** systems (as Cartesian coordinates). This material is available free of charge via the Internet at <http://pubs.acs.org>.

JA0291181

- (25) Frisch, M. J.; Trucks, G. W.; Schlegel, H. B.; Scuseria, G. E.; Robb, M. A.; Cheeseman, J. R.; Zakrzewski, V. G.; Montgomery, J. A., Jr.; Stratmann, R. E.; Burant, J. C.; Dapprich, S.; Millam, J. M.; Daniels, A. D.; Kudin, K. N.; Strain, M. C.; Farkas, O.; Tomasi, J.; Barone, V.; Cossi, M.; Cammi, R.; Mennucci, B.; Pomelli, C.; Adamo, C.; Clifford, S.; Ochterski, J.; Petersson, G. A.; Ayala, P. Y.; Cui, Q.; Morokuma, K.; Malick, D. K.; Rabuck, A. D.; Raghavachari, K.; Foresman, J. B.; Cioslowski, J.; Ortiz, J. V.; Stefanov, B. B.; Liu, G.; Liashenko, A.; Piskorz, P.; Komaromi, I.; Gomperts, R.; Martin, R. L.; Fox, D. J.; Keith, T.; Al-Laham, M. A.; Peng, C. Y.; Nanayakkara, A.; Gonzalez, C.; Challacombe, M.; Gill, P. M. W.; Johnson, B.; Chen, W.; Wong, M. W.; Andres, J. L.; Gonzalez, C.; Head-Gordon, M.; Replogle, E. S.; Pople, J. A. Gaussian, Inc.: Pittsburgh, PA, 1998.
- (26) (a) Parr, R. G.; Yang, W. *Density Functional Theory of Atoms and Molecules*; Oxford University Press: Oxford, United Kingdom, 1989. (b) Ziegler, T. *Chem. Rev.* **1991**, *91*, 651.
- (27) (a) Lee, C.; Yang, W.; Parr, R. G. *Phys. Rev. B* **1988**, *37*, 785. (b) Becke, A. D. *J. Chem. Phys.* **1993**, *98*, 5648. (c) Stephens, P. J.; Devlin, F. J.; Chabalowski, C. F.; Frisch, M. J. *J. Phys. Chem.* **1994**, *98*, 11 623.
- (28) Hay, P. J.; Wadt, W. R. *J. Chem. Phys.* **1985**, *82*, 299.
- (29) Höllwarth, A.; Böhme, M.; Dapprich, S.; Ehlers, A. W.; Gobbi, A.; Jonas, V.; Köhler, K. F.; Stegmann, R.; Veldkamp, A.; Frenking, G. *Chem. Phys. Lett.* **1993**, *208*, 237.
- (30) (a) Francl, M. M.; Pietro, W. J.; Hehre, W. J.; Binkley, J. S.; Gordon, M. S.; Defrees, D. J.; Pople, J. A. *J. Chem. Phys.* **1982**, *77*, 3654. (b) Hehre, W. J.; Ditchfield, R.; Pople, J. A. *J. Chem. Phys.* **1972**, *56*, 2257. (c) Hariharan, P. C.; Pople, J. A. *Theor. Chim. Acta* **1973**, *28*, 213.

- (31) Peng, C.; Ayala, P. Y.; Schlegel, H. B.; Frisch, M. J. *J. Comput. Chem.* **1996**, *17*, 49.
- (32) Allinger N. L. *MM3(92)*; QCPE: Bloomington, Indiana, 1992.
- (33) Rappé, A. K.; Casewit, C. J.; Colwell, K. S.; Goddard, W. A., III.; Skiff, W. M. *J. Am. Chem. Soc.* **1992**, *114*, 10 024.